Received: 2 October 2018 | Revised: 18 June 2019 | Accepted: 20 June 2019
DOI: 10.1002/we.2394

WILEY

RESEARCH ARTICLE

Effect of foundation type and modelling on dynamic response and fatigue of offshore wind turbines

Ingrid B. Løken[1] | Amir M. Kaynia[2,3]

[1]DNV GL AS, Oslo, Norway
[2]Norwegian University of Science and Technology (NTNU), Trondheim, Norway
[3]Norwegian Geotechnical Institute (NGI), Oslo, Norway

Correspondence
Amir M. Kaynia, Norwegian University of Science and Technology (NTNU), Trondheim, Norway.
Email:amir.kaynia@ntnu.no

Abstract

This paper presents dynamic response and fatigue analyses of several bottom-mounted *offshore wind turbine* (OWT) models, simulated in the aero-hydro-servo-elastic simulation tool FAST. The distinction between the models is the foundations, which are modelled with different methods, concepts, and dimensions. The US National Renewable Energy Laboratory has developed a 5-MW reference turbine supported on a monopile, the *NREL 5MW*, which was used as a reference model in this paper. The paper presents the implementation and comparison of two different foundation modeling methods, referred to as the *simplified apparent fixity method* and the *improved apparent fixity method*. Furthermore, sensitivity analyses of different monopile dimensions were performed, followed by sensitivity analyses of suction caisson foundations of different dimensions. The final part of the paper presents fatigue analyses for the foundation models considered in this study subjected to 17 load cases. Fatigue damage, fatigue life, and damage equivalent loads were calculated, as well as the relative fatigue contribution from each load case.

KEYWORDS

apparent fixity, FAST, foundation, modelling, monopile, wind turbine

1 | INTRODUCTION

The global focus on utilizing renewable energy sources is constantly increasing. The offshore wind industry has grown remarkably over the past few years. This growth has brought global offshore wind capacity to over 20 GW.[1]

An important research area within offshore wind turbines (OWTs) is the response of different foundations. Monopile is by far the most common foundation type and accounts for over 80% of all installed OWTs.[2] However, new concepts for larger water depths, such as suction caissons, multi-piles, and moored floating structures, are being investigated. Despite this, the monopile is expected to continue to have a large market share in the years to come.

The harsh environmental conditions make design and construction of offshore turbine foundations challenging. The foundations must take account of turbine weight and height, the depth of water, the wind load, wave and current loads, and the special soil conditions at the particular site. Knowledge about the dynamics of the whole wind turbine structure-foundation system is important for predicting the dynamic response and fatigue damage.

Soil-Structure Interaction (SSI) plays a major role in the response of bottom-mounted OWTs. Nevertheless, modelling of the foundation is still crude in most wind turbine simulation codes.[3] In FAST, which is the software used in this study, the default OWT model is limited to a rigid connection below the seabed. Inclusion of the soil-foundation flexibility would give a softer model, which reduces the natural frequencies of the OWT system and decreases fatigue. Improved knowledge of the foundation modelling and foundation concepts will likely lead to reduced fatigue damage or result in dimension reductions, which are both highly economically attractive.

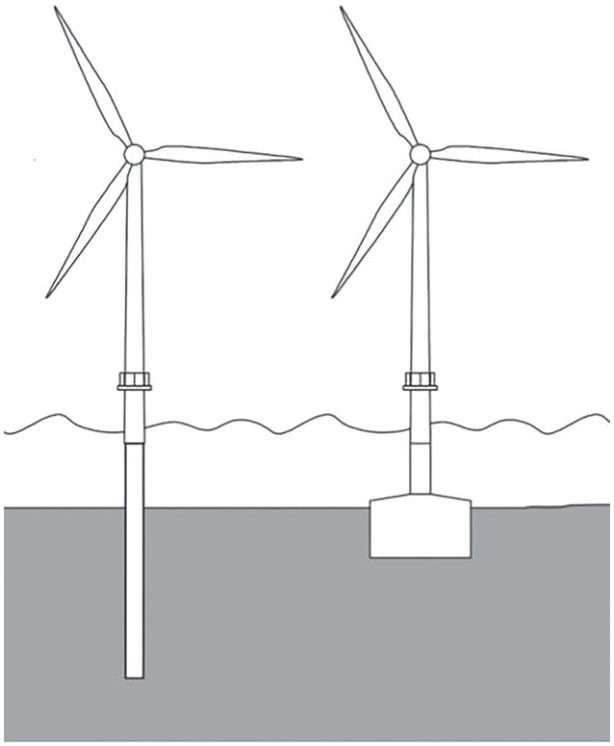

FIGURE 1 OWT with a monopile foundation (left) and a caisson foundation (right)

The objectives of this paper are to assess the impact of (a) different foundation modelling methods, (b) foundation dimensions, and (c) different foundation concepts with respect to dynamic response and fatigue damage of a typical megawatt-size OWT structure.

1.1 | OWT foundations

OWTs are slender structures that are exposed to large overturning moments at the base. Several foundations concepts exists for bottom-mounted OWTs. This paper focuses on the monopile and the caisson foundation, shown in Figure 1.

Monopiles are still the most commonly used foundation type due to their simplicity of installation and long and successful experience of their use in oil and gas platforms.[4] The suction caisson is considered a suitable foundation solution in OWT jackets in deeper water. It is installed by negative pressure when the water inside is pumped out. The main advantages of the suction caisson are the ease of installation and its relatively light weight.[5]

1.2 | Review of OWT foundation modelling

SSI has traditionally been handled using foundation impedances that give relationships between the loads (forces and moments) and the corresponding responses (displacements and rotations) at the foundation-structure interface. For linear elastic soil response, analytical solutions have been developed for a variety of foundations, such as piles and surface foundations, and for different soil types. Some of these solutions also provide the variation of the foundation impedances with frequency. See Kausel[6] for a review of these solutions. For structural loads leading to slight soil nonlinearities, these solutions have been used by using strain-compatible elastic moduli of the soil. For larger loads leading to non-negligible soil nonlinearity or even near-failure conditions, the classical solutions based on fully integrated soil- foundation-structures models in finite elements have been the preferred approach.[7] However, given the simplicity and computational-efficient character of the solutions based on foundation impedances, there has been a great interest in extending them to the nonlinear range. For such conditions, the terminology has changed to macro-elements. In simple terms, macro-elements represent the nonlinear load-response of the foundation, covering small to large load levels. Macro-elements have in particular been popular in shallow foundations such as caissons and bucket foundations that are becoming more common in OWTs.[8]

While the impedance approach has long been used for piles in the elastic range (eg, Novak and Nogami,[9] Kaynia,[10] and Kaynia and Kausel[11]), soil-pile interaction has for practical reasons been handled by the use of Winkler springs along the pile.[12] These springs were first used in design of piles for offshore platforms, using the terminology of p-y curves,[13] thanks to the data collected from field tests on piles. With the introduction of large monopiles in OWT design, new simplified methods have become more common. According to Passon and Kühn,[3] the most common models used for monopiles are (a) *apparent fixity* (AF) model in which the monopile is extended to a certain depth below the seabed and is rigidly fixed there, (b) single element model in which the tower model is assumed rigid and mounted on a set of springs and dampers at the pile

head, and (c) distributed element model, where the soil is represented by a series of springs along the length of the pile as in the well-known p-y curves.

A large number of research has been carried out to investigate the interaction between the soil and monopiles in OWTs. Zaaijer[14] used simplified dynamic models for monopiles and compared the first and second bending modes of the pile. The reference model for the soil-monopile interaction was the Winkler distributed spring.[12] This model was compared with those based on the apparent fixity, stiffness matrix of the pile at the seabed level, and uncoupled pile-head springs. The author concluded that the stiffness-matrix approach outperforms the other two models. Bush and Manuel[15] used similar models of monopile foundation in their investigation of the effect of extreme loading. They compared the fixed base model with the apparent fixity model and a distributed element model with linear elastic springs along the monopile. They concluded that the long-term extreme loads for the apparent fixity and the distributed element model are larger compared with the fixed base model. Klinkvort[16] simplified the elastoplastic model initially proposed by Boulanger et al[17] by implementing a procedure to account for the gap developed between the monopile and the soil at large loads. Following these ideas, Taciroglu et al[18] proposed a model using three components: leading-face element, rear-face element, and drag-element. Schløer[19] used a similar model to investigate the response of OWTs subjected to linear and nonlinear waves and highlighted the importance of the wave nonlinearity in the design of the OWTs.

Zania[20] followed the approach of Novak and Nogami[9] by using the substructuring method[6] and computed the dynamic response of soil-pile interaction. She implemented an iterative two-step analytical method that allows consideration of the off-diagonal terms of the dynamic impedance matrix. The results highlighted the importance of using the frequency-dependent impedances and the off-diagonal impedance terms on the natural frequencies and the damping of the system. Ziegler et al[21] also developed a frequency-domain solution based on the Winkler approach in order to calculate wind-induced fatigue in OWTs on monopiles. Their sensitivity analyses showed that water depth and wave period have important influence on the fatigue loads. Most recently, Markou and Kaynia[22] developed a procedure for extending the non-linear static p-y springs to cyclic loading and implemented a procedure for limiting the damping generated by the hysteretic loops in the springs. To assess the importance of soil-pile modelling and damping, Aasen et al[23] carried out a parametric study in which they used four different models for the simulation of the monopile of an OWT. The first model, which is a common model used in the industry, comprised nonlinear elastic springs that do not dissipate energy; the second model was a linear elastic stiffness matrix at the pile head; the third model was similar to the second one with the addition of damping, and the last model consisted of uncoupled nonlinear horizontal and rotational springs at the pile head represented by a series of elasto-plastic springs as proposed by Iwan.[24] The authors concluded that the the first model is conservative for the estimation of the fatigue damage of the system while the last model, which is the most realistic of the models, reduces fatigue damage and could provide a more economical design.

Krathe and Kaynia[25] implemented a nonlinear macro-element foundation model in FAST v7.[26] The macro-element represents the nonlinear force-displacement (or moment-rotation) relationship at the pile head. The nonlinear response can then be captured by the combination of parallel elasto-plastic springs proposed by Iwan.[24] The authors highlighted the importance of nonlinear soil response and damping which is captured by this model.

Bisoi and Haldar[27] performed an extensive finite element study on the dynamic response of an OWT monopile modelled with nonlinear foundation Winkler model. They concluded that the response of the overall system is affected by the interaction between the foundation and the superstructure, the soil nonlinearity, the rotor frequency, and the magnitude of wave load. Carswell et al[28] used FAST together with a specialized finite element code for the computation of foundation damping in order to investigate the effect of modelling on the first natural frequency of a monopile-supported OWT under extreme storm loading. The monopile foundation was simulated with a lumped-parameter model at the pile head. They concluded that foundation damping decreases the moment at the mudline level under extreme storm conditions and should be considered for more economical design.

Bayat et al[29] studied the impact of drained and undrained soil behavior on the stiffness and damping of soil- pile interaction of OWT monopiles. They use a simple Kelvin model in a two-dimensional finite element program to simulate a segment of a monopile at different depths subjected to small-magnitude cyclic loading. The authors used the results and presented effective stiffness and equivalent damping diagrams of the soil that can be applied to p-y-y' models of the Kelvin type.

Aasen[30] studied the influence of SSI on the fatigue damage of a monopile supported OWT. Three different foundation models where studied, and the fatigue analyses showed significant decreases in accumulated fatigue damage in the pile as soil damping where introduced. Damgaard et al[31] used a frequency-domain solution to compute the dynamic impedances of the pile-soil system and calibrated a lumped-parameter model for integration into an aeroelastic code. In addition to the lumped-parameter model, they used two other models for the monopile foundation, namely, the apparent fixity and the fixed support model at the seabed level. The authors concluded that soil-pile interaction is important for the design in terms of fatigue at the seabed level. Andersen et al[32] used a finite difference solution to estimate the response of OWTs on a simple Winkler model calibrated using p-y curves. They concluded that a reliable estimation of the first natural frequency of the system is crucial for the assessment of the fatigue damage of the system.

A number of studies have been carried out on the stiffnesses of suction caissons using a variety of numerical and analytical solutions (eg, Pais and Kausel[33]; Doherty et al[34]; Liingard et al[35]; Gelagoti et al[36]; He et al[37]; Efthymiou and Gazetas[38]). These studies have covered homogeneous and nonhomogeneous soil media and have included linear and nonlinear soil behavior.

Rating	5 MW
Rotor orientation, configuration	Upwind, 3 blades
Rotor diameter, hub diameter	126 m, 3 m
Hub height	90 m
Cut-in, rated, cut-out wind speed	3 m/s, 11.4 m/s, 25 m/s
Cut-in, rated rotor speed	6.9 rpm, 12.1 rpm
Rated tip speed	80 m/s
Rotor mass	110 000 kg
Nacelle mass	240 000 kg
Tower mass	347 460 kg
Tower height	87.6 m
Tower top diameter, wall thickness	3.87 m, 0.019 m
Tower base diameter, wall thickness	6.0 m, 0.027 m
Substructure base diameter, wall thickness	6.0 m, 0.06 m
Support structure steel density	8500 kg/m^3
Steel Young modulus	210 GPa
Steel Shear modulus	80.8 GPa
Support structure structural-damping ratio (all modes)	1 %

TABLE 1 Properties of the NREL 5-MW baseline wind turbine

1.3 | Computational tool: FAST

The software used to model the OWT in this study is FAST.[26] It is an open-source aero-hydro-servo-elastic CAE (Computer Aided Engineering) tool for modelling horizontal axis wind turbines (HAWT), developed by the National Renewable Energy Laboratory (NREL) through the US Department of Energy (DOE). FAST v8 was used in this study.[39] The FAST modules used were *SubDyn* and *ElastoDyn* for the structural dynamics, *ServoDyn* for the power generation, and *InflowWind*, *HydroDyn*, and *AeroDyn* for external conditions and applied loads.

FAST employs a combined modal and multibody dynamics formulation. The multibody formulation applies to the support platform, nacelle, generator, gears, hub, and tail, while the modal formulation applies to the blades and the tower. FAST relies on an assumed modes approach, implying that the blade and tower mode shapes are required as input. The software used to compute the mode shapes is the finite element code *BModes*,[40] which is not yet a part of the FAST modularization framework and needs to be run separately.

1.4 | NREL 5MW baseline wind turbine

NREL has developed a reference turbine with detailed specifications representative of a typical utility-scale multi-megawatt turbine, known as the *NREL 5-MW offshore baseline wind turbine*. It is a three-bladed upwind HAWT with a monopile support structure, developed for researches to have a common reference model for studies of OWTs. It has been used in several international research projects and is also used in this study. The specifications of the turbine are listed in Table 1[41] for completeness.

The substructure has a fixed boundary at the base, which means that neither lateral nor rotational movements are allowed there. This model will subsequently be referred to as the fixed base model.

2 | FOUNDATION MODELS

The following sections present the standard approach for foundation modelling of OWTs in FAST, known as the Apparent Fixity method, and a proposed improvement for more accurate foundation representation.

2.1 | Apparent fixity method

Impedances of all types of foundations that are computed by rigorous analytical or advanced numerical models can be expressed in the horizontal vibration mode as 2 x 2 coupled matrices (ie, with nonzero off-diagonal terms). Methods for modelling the foundation with either coupled matrices, uncoupled springs, or distributed springs are not available in FAST v8 and thus require modification of the source code. Therefore, the method used in this paper to model flexibility of the soil-foundation system is based on an extension of the apparent fixity (AF) method available in FAST. In the AF method, the foundation flexibility is represented by inclusion of a beam with fixed base below the mudline.

In this section, the principle of the AF method is described briefly as background to an extension introduced in the next section. The principle behind the AF method is shown schematically in Figure 2.

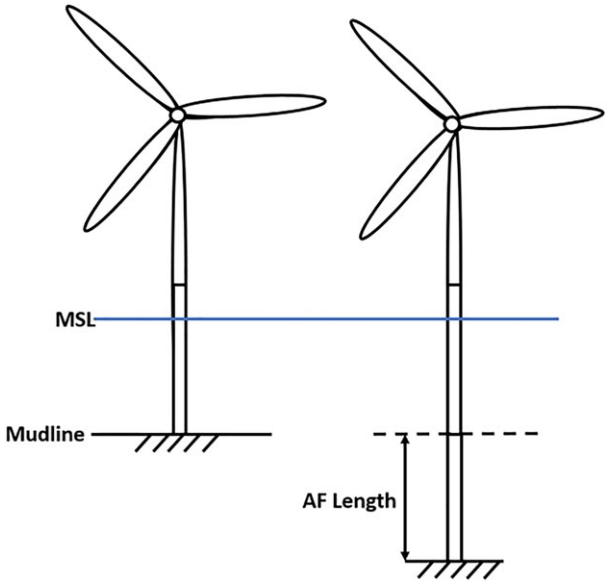

FIGURE 2 Fixed-base foundation model (left) and flexible foundation model using the apparent fixity method (right) [Colour figure can be viewed at wileyonlinelibrary.com]

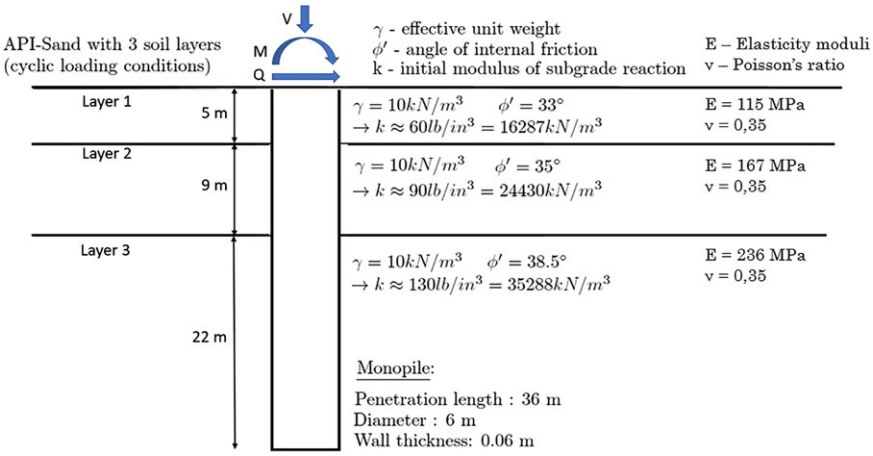

FIGURE 3 The soil profile from which the foundation stiffness matrix was derived [Colour figure can be viewed at wileyonlinelibrary.com]

The length, L_{AF}, and bending rigidity, EI_{AF}, of the fictive AF beam are calculated such that the stiffness matrix of the AF beam is identical to the 2 x 2 impedance matrix of the soil-foundation system as given in Equation (1):

$$K = \begin{bmatrix} k_{uu} & k_{u\theta} \\ k_{\theta u} & k_{\theta\theta} \end{bmatrix} = \begin{bmatrix} \frac{12EI_{AF}}{L_{AF}^3} & -\frac{6EI_{AF}}{L_{AF}^2} \\ -\frac{6EI_{AF}}{L_{AF}^2} & \frac{4EI_{AF}}{L_{AF}} \end{bmatrix}, \quad (1)$$

where k_{uu} is the horizontal stiffness, $k_{\theta\theta}$ is the rotational stiffness, and $k_{u\theta} = k_{\theta u}$ are the coupled stiffness terms.

To compute the stiffness terms in Equation (1) and the parameters of the AF beam, the properties of the real monopile and the soil surrounding it are needed. The monopile penetration depth of the NREL 5MW was set to 36 m,[42] and the soil profile is the one described by Passon,[43] shown in Figure 3.

Passon[43] and Bush et al[44] present studies of foundation models for the NREL 5MW using the soil profile in Figure 3. Both these studies used a nonlinear soil-pile lateral analysis programme to calculate deflection u and rotation θ at the mudline for specified levels of shear force F and moment M. An interesting observation[44] was that L_{AF} and EI_{AF} were only slightly affected by different load cases. This suggests that the soil behavior is almost linear for the pile and soil properties studied here for the range of simulated environmental loads. Hence, it was chosen in the present study to use the linear soil-pile analysis software PILES[45] to calculate the stiffness of the soil-pile system in Figure 3. The inputs required by PILES are the soil moduli and Poisson's ratios of the soil layers, which are indicated in Figure 3, and the pile's elastic parameters. The elastic moduli of the soil layers were estimated using the analytical formula derived by Vesic[46] expressing the coefficient of subgrade modulus, k, as a function of the pile diameter, the pile's bending rigidity and the elastic modulus and Poisson's ratio of the soil layer. For the subgrade modulus, k, indicated for each layer in Figure 3, the associated elastic modulus was computed by Vesic's formula and is included in Figure 3. The soil below the third layer (ie, below pile tip) was assumed a half space with properties similar to those of the third layer. PILES is an elasto-dynamic code which uses the Green's functions in layered half-space for capturing the soil response to the pile-soil tractions together with the analytical equations of the piles modelled as a beam. The output of PILES is a 6 x 6 stiffness matrix of the pile at the mudline, representing the stiffness

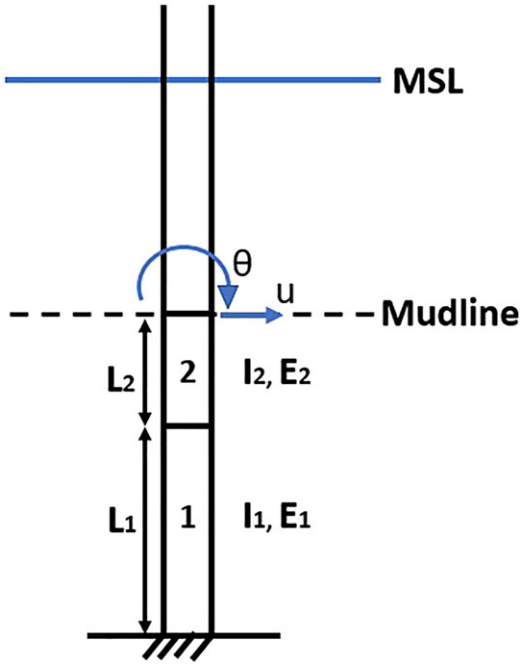

FIGURE 4 Improved apparent fixity method [Colour figure can be viewed at wileyonlinelibrary.com]

terms of the soil-pile system in the two horizontal DOFs, the vertical DOF, two rotational DOFs, and one torsional DOF. Soil behavior is assumed to be isotropic, which implies that the stiffness matrix in the two horizontal directions, surge and sway, are identical. The 2 x 2 stiffness matrix in the two directions, which governs the lateral dynamic response of the OWT, is given in Equation (2):

$$[K]_{PILES} = \begin{bmatrix} k_{uu} & k_{u\theta} \\ k_{\theta u} & k_{\theta\theta} \end{bmatrix} = \begin{bmatrix} 2.84 \times 10^{9} & -1.56 \times 10^{10} \\ -1.56 \times 10^{10} & 1.93 \times 10^{11} \end{bmatrix}. \quad (2)$$

The units of k_{uu}, $k_{u\theta}$, $k_{\theta u}$, and $k_{\theta\theta}$ are N/m, N/rad, Nm/m, and Nm/rad, respectively.

The common practice in geotechnical research and engineering is to match only the diagonal stiffness terms (3) while neglecting the off-diagonal terms. Due to this simplification, the method described in this section is referred to as the *simplified AF method*.

After calculating L_{AF} and EI_{AF} from the stiffness terms, these were implemented in the SubDyn input file in FAST. The structural damping, given as a percentage of critical damping, was kept the same as in the rest of the structure, ie 1%, following the recommendations of DNV GL.[47] The material density was kept the same as the substructure above the mudline.

2.2 | Improved apparent fixity method

In order to investigate whether the simplified AF method gives acceptable results for large piles like OWT monopiles, an improved model method was developed. The objective was to study the effect of the coupled stiffness terms on the dynamic response of the reference OWT.

One solution to accurately reproduce the whole stiffness matrix is by introducing a rigid link with a length equal to $k_{u\theta}/k_{uu}$ under the tower at the mudline and placing it on horizontal and rotational springs corresponding to the diagonal terms of the monopile stiffness. This method is described by Carswell et al[28] and is applicable to FAST v7. However, it is not possible to implement springs in FAST v8. Therefore, a second method was developed in this paper, which enables exact reproduction of the stiffness matrix of the monopile. This was done by replacing the single AF beam described in Section 2.1 with *two* beams, creating a system of three equations with three unknowns, including the off-diagonal stiffness terms in the equation system. This new method of including foundation flexibility in the OWT model, referred to as the *improved apparent fixity method* or simply the *improved AF method*, is explained below and was implemented in FAST.

Two beams are added below the mudline to correctly represent the stiffness matrix of the true soil-pile system. Beam 1 is rigidly connected to a certain point below the mudline and to beam 2, which is rigidly connected to the base of the substructure (Figure 4).

Considering that the lateral dynamic response of the tower is governed by bending of the structure, the vertical and torsional DOFs, as described in Section 2.1, can be ignored and the two-beam system is reduced to a two-dimensional system with two DOFs; deflection u and rotation θ at the mudline. There are several ways of solving this system. The chosen method here consists of obtaining a flexibility matrix $[F]$ at the mudline and setting it equal to the flexibility matrix from PILES, $[F]_{PILES}$, representing the true soil-pile system. $[F]_{PILES}$ was found from the stiffness matrix presented in Section 2.1 through the following relation:

$$[F]_{PILES} = [K]^{-1}_{PILES} = \begin{bmatrix} 6.33 \times 10^{-10} & 5.12 \times 10^{-11} \\ 5.12 \times 10^{-11} & 9.32 \times 10^{-12} \end{bmatrix}. \quad (3)$$

It can be shown that the flexibility matrix [F] of the two beam system in Figure 4 is given by Equations (4) to (7).[48]

$$[F] = \begin{bmatrix} \delta_{uu} & \delta_{u\theta} \\ \delta_{\theta u} & \delta_{\theta\theta} \end{bmatrix}, \tag{4}$$

where

$$\delta_{uu} = \frac{1}{E_1 I_1}\left(\frac{L_1^3}{3} + L_1^2 L_2 + L_2^2 L_1\right) + \frac{L_2^3}{3E_2 I_2}, \tag{5}$$

$$\delta_{u\theta} = \delta_{\theta u} = \frac{1}{E_1 I_1}\left(\frac{L_1^2}{2} + L_1 L_2\right) + \frac{L_2^2}{2E_2 I_2}, \tag{6}$$

$$\delta_{\theta\theta} = \frac{L_1}{E_1 I_1} + \frac{L_2}{E_2 I_2}. \tag{7}$$

There are different combinations of the parameters of the two beams that could give the desired flexibility terms. In the present work, the diameter and wall thickness of the two beams were kept the same as for the monopile at the mudline, ie, 6 and 0.06 m, respectively, which implies that the area moment of inertia is known, and $I_1 = I_2 = I$. Assigning a value to the length of the upper beam L_2 leaves the length of the lower beam, L_1, and the Young's modulus of the two beams, E_1 and E_2, as the three unknown parameters. Table 2 lists the parameters computed by this procedure.

The new system was implemented in SubDyn as two beam members below the mudline with the properties from Table 2 and the boundary conditions from Figure 4. All the DOFs of the lower end of beam 1 were constrained to make it rigidly connected to a point at a distance $L_1 + L_2$ below the mudline.

2.3 | FAST simulations

FAST simulations were run for the fixed-base model, the simplified AF model, and the improved AF model of the 5MW NREL turbine. A full-field turbulent wind field was generated by TurbSim, using the Kaimal spectral model[47] with a mean wind velocity U of 12 m/s and turbulence intensity $TI = 14$ %. The hydrodynamic loads were generated by HydroDyn, using an irregular JONSWAP wave spectrum, including consideration of second-order sum-frequency hydrodynamic effects. The significant wave height H_s was set to 6 m and spectral wave period T_p was set to 10 seconds. The runtime was 630 seconds. A time window of the mudline moment in the fore-aft direction for the three foundation models is shown in Figure 5.

The figure illustrates how significant small adjustments in the implementation of the foundation model can be. Surprisingly, the off-diagonal terms of the soil-foundation stiffness matrix play an important role, and neglecting them results in a model that is too soft. It is clear from Figure 5 that the simplified AF method overpredicts the loads in the structure. It is shown by Løken[48] that these differences are significantly amplified when the wave periods are decreased towards the operational and structural natural frequencies of the OWT.

New simulations with only white noise load were run to obtain the *power spectral densities* (PSDs), which are plotted in Figure 6. The PSDs illustrate that the natural frequencies of the improved AF model are between the values of the fixed base model and the simplified AF model.

3 | SENSITIVITY ANALYSES WITH MONOPILE

It is believed in the OWT community that the monopile foundations in most of currently operating OWTs have conservative designs. Increased accuracy in foundation modelling in OWT analyses and simulation codes backed by observed full-scale measurements has lead to more reliable models supporting the reduction of foundation dimensions and hence remarkable cost reductions.

TABLE 2 Properties of the two AF beams

Beam Number	L, m	d, m	t_w, m	I, m^4	E, N/m^2
1	19.88	6.00	0.06	5.089	1.743×10^{12}
2	5.00	6.00	0.06	5.089	1.388×10^{11}

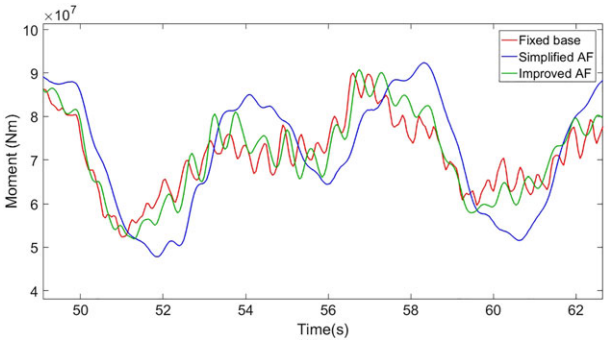

FIGURE 5 Mudline moment oscillations for the three foundation models [Colour figure can be viewed at wileyonlinelibrary.com]

In this section, limited sensitivity analyses of the NREL 5MW monopile foundation with different dimensions are presented. The monopile length and wall thickness were changed to assess their effects on the structural response. The new foundation properties were implemented in SubDyn using the improved AF method, and a 10-minute FAST simulation with $U = 12$m/s, $TI = 14\%$, $H_s = 6$ m and $T_p = 10$s was run for each model. The regular monopile with pile wall thickness $t_w = 0.06$ m and pile length $L = 36$ m modelled through the improved AF method will in the following be referred to as the *regular monopile* or just the *monopile*.

3.1 | Effect of pile length

Two foundation models with reduced monopile lengths were simulated: one with a length of 26 m and one with a length of 16 m. The rest of the OWT model and the soil profile were kept the same. Implementing the new lengths in PILES shows that even this large reduction in pile length has only a minor effect on the stiffness. Consequently, the properties of the fictive AF beams below the mudline do not change significantly for the three models. Nevertheless, the AF properties were implemented in SubDyn, and FAST simulations of the three models were run. The mudline fore-aft bending moment is plotted in Figure 7.

Figure 7 clearly demonstrates that the applied reduction in monopile length does not make a noticeable difference in the structural dynamic response. However, it should be noticed that this result does not imply that the pile can be designed to be 26 or 16 m instead of 36 m. In addition to structural response, in a comprehensive design, the designer must check a number of issues such as the soil and structural capacity, the permanent tilt, and other performance requirements. The present sensitivity study only considered the overall dynamic response and performance in terms of a limited fatigue evaluation (see Section 5).

3.2 | Effect of pile wall thickness

Two new models of the monopile were simulated, in which the wall thickness was changed from $t_w = 0.06$ m to $t_w = 0.05$ m, and $t_w = 0.04$ m. Capacity and other design issues, as discussed in Section 3.1, are not considered in this sensitivity study, the focus is rather on the overall dynamic response. The new pile parameters were implemented in PILES, and the resulting stiffness coefficients for the three models are presented in Table 3.

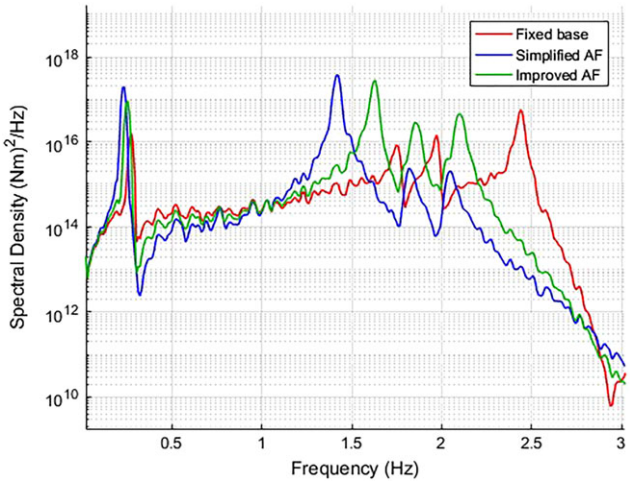

FIGURE 6 PSD from fore-aft mudline moment for the fixed base model, the simplified AF model and the improved AF model [Colour figure can be viewed at wileyonlinelibrary.com]

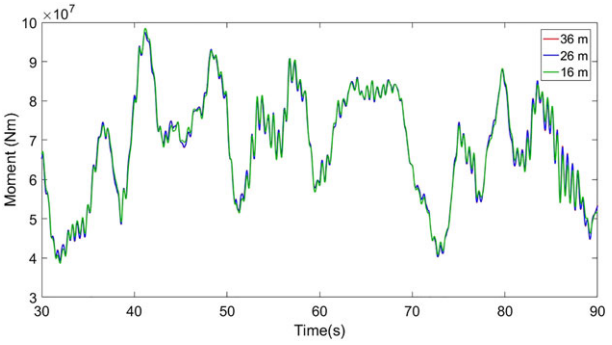

FIGURE 7 Fore-aft mudline moment for models with different monopile lengths [Colour figure can be viewed at wileyonlinelibrary.com]

TABLE 3 Stiffness coefficients from PILES for different pile wall thickness

Pile Wall Thickness	k_{uu}, N/m	$k_{u\theta}$, N/rad	$k_{\theta\theta}$, Nm/rad
$t_w = 0.06$ m	2.84×10^9	-1.56×10^{10}	1.93×10^{11}
$t_w = 0.05$ m	2.74×10^9	-1.43×10^{10}	1.68×10^{11}
$t_w = 0.04$ m	2.61×10^9	-1.28×10^{10}	1.43×10^{11}

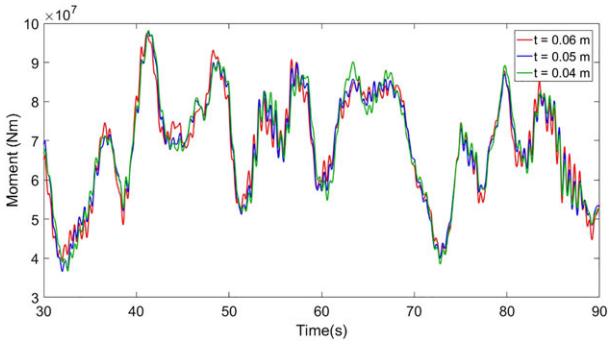

FIGURE 8 Fore-aft mudline moment for the models with different wall thickness [Colour figure can be viewed at wileyonlinelibrary.com]

TABLE 4 Maximum response values from FAST simulations of the models with different pile wall thickness

	Tower Top Displacement		Mudline Moment		Mudline Stress	
Wall thickness	Max Value, m	%	Max Value, MNm	%	Max Value, MPa	%
t_w = 0.06 m	0.813	0.0	115.8	0.0	68.4	0.0
t_w = 0.05 m	0.901	+11%	116.7	+1%	82.6	+21%
t_w = 0.04 m	1.013	+25%	120.0	+4%	106.0	+55%

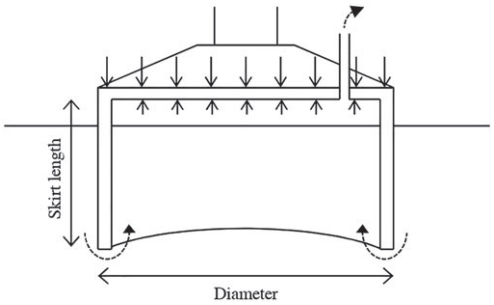

FIGURE 9 Caisson foundation principle sketch

The computed parameters of the improved AF model were implemented in the SubDyn input file, and FAST simulations were run. The time series from 30 to 90 seconds of mudline moment is plotted in Figure 8.

Even though the moments are fairly close, there are large differences in bending stress due to the reduction of moment of inertia *I*. The maximum values for the tower top displacement and mudline bending moment from the simulations above are listed in Table 4, along with the maximum bending stresses at the mudline. The percentage differences between the reduced thickness models compared with the regular monopile are also presented.

The reduced wall thickness has a large effect on the bending stress in the structure. This will clearly have a high impact on the fatigue damage of the structure, which is studied in Section 5.

4 | CAISSON FOUNDATIONS

With the purpose of comparing the dynamic response and fatigue life of different foundation concepts, modelling of caisson foundations using the improved AF method is considered in this section.

As the turbine sizes and water depths increase, production and installation of large-diameter monopiles become more challenging, partly due to the need for heavy installation vessels and equipment. The suction caisson, also called *suction bucket* or *monopod*, originally developed for the foundation of offshore oil platforms, is an alternative to the monopile. It has the advantages of being easy to install and remove, is suitable for deeper water depths (up to 55 m), and requires less steel than a comparable monopile.

The suction caisson is a cylindrical skirted foundation, attached to the base of the substructure, and inserted into the seabed. It consists of a circular top plate whose strength and stiffness are enhanced by peripheral stiffeners over the top plate and embedded skirts which confine the internal soil (Figure 9). The caisson is driven into the seabed by means of self-weight and by pumping out the water trapped inside it. The induced pressure difference creates suction, which pushes the skirts into the soil.[7] After installation, it behaves as a skirted foundation that utilizes the friction between the skirts and the soil and the pressure below the top plate.

In this section, simplified models of caisson foundations with different dimensions supporting the NREL 5MW are implemented in FAST. As discussed earlier, a reduction in foundation dimensions will be highly favorable in the offshore wind industry. Therefore, sensitivity analyses consisting of varying the diameter and depth of the caisson are presented here.

Caisson Dimensions	k_{uu}, N/m	$k_{u\theta}$, N/rad	$k_{\theta\theta}$, Nm/rad
15 × 7.5 m	5.54×10^{9}	-2.96×10^{10}	5.05×10^{11}
12 m × 6 m	4.08×10^{9}	-1.77×10^{10}	2.46×10^{11}
10 m × 5 m	3.17×10^{9}	-1.14×10^{10}	1.35×10^{11}

TABLE 5 Stiffness coefficients from G123 for different caisson dimensions

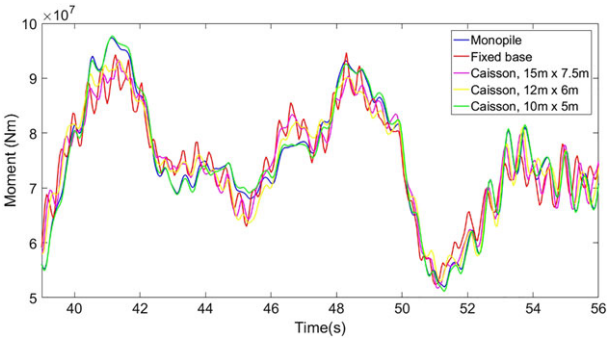

FIGURE 10 Time window of mudline fore-aft bending moment for different caisson dimensions, compared with the regular monopile and the fixed base model [Colour figure can be viewed at wileyonlinelibrary.com]

In order to model the caisson foundations, the same approach was used as for the monopile, namely, the stiffness matrix of the soil-foundation system was computed at the mudline, and was represented through the improved AF method.

The same soil profile as in the previous sections was used. The rigorous elasto-dynamic program G123[49] was used to obtain the stiffness matrix of the soil-caisson system at mudline. G123 is an elasto-dynamic code for computation of the dynamic impedances of rigid circular foundations in layered soil. It is based on the solution of the wave propagation equations using the mode shapes of a stratum and perfectly absorbing boundaries. The required inputs to G123 are the radius of the caisson, shear modulus G, Poisson's ratio ν, and damping of both the soil layers and the foundation. G123 assumes the foundation to be a solid shallow footing, implying that the input properties have to be set to include the soil confined by the bucket skirts. Ideally, an FE model of the caisson should be made to obtain the representative properties. However, previous analyses of caisson foundations show that, due to the internal stiffeners and incompressible soil in the compartments, they are indeed very stiff. With that in mind, the shear modulus G of the caisson was set as 1000 times larger than the shear modulus of the soil outside. Because G123 is based on a formulation with fixed boundary at the bottom of the soil domain, the base of the soil model in Figure 3 was fixed at a large depth.

It was assumed that the caisson foundation is rigidly connected to the substructure of the NREL 5MW at the mudline. That is, possible stiffeners between the caisson and the monopile were not considered. The rest of the OWT above the foundation was kept the same as the original model.

The first prototype of a caisson foundation was installed in 2002 in Fredrikshavn, supporting a 3 MW Vestas V90 turbine in 4-m water depth. To further demonstrate that the caisson foundation could be successfully installed offshore, prototypes supporting meteorological masts have been installed at the Horns Rev 2 offshore project (2009) and the Dogger Bank project (2013). The Fredrikshavn and Horns Rev 2 caisson have a diameter of 12 m and a skirt length of 6 m. As a starting point, this size was used as the reference model. In addition, two caissons with dimensions 12 m × 6 m and 15 m × 7.5 m were also modelled. The caisson models were run in G123, and the calculated stiffness coefficients are listed in Table 5.

Table 5 shows that the caisson foundation with diameter D_c = 10 m and depth L_c = 5 m have a rocking stiffness approximately equal to the standard monopile. The improved AF model parameters were calculated using Equations (5), (6), and (7), as before.

A total of 630-second FAST analyses were run for the different models with the same load case as in Section 2.3. Like the monopile, the caisson will experience large moment and horizontal loads, particularly at the mudline. Figure 10 shows time histories of the mudline fore-aft bending moments for models of the NREL 5MW supported by monocaissons with different dimensions. The results for both the monopile and the fixed-base model are included for comparison. The fact that the maximum moments in these cases are fairly similar indicates that the tower response is not largely affected by the dynamic effects due to SSI.

As was discussed in Section 3, the sensitivity analyses made in this paper do not consider all aspects of design, like capacity and buckling, which can be important issues in thin-walled structures.[50] Nevertheless, the results are meant to compare the dynamic response and, in the next section, the relative fatigue life of the different foundation models are studies.

The mean and maximum values for the mudline moments, mudline shear force, and tower top displacement in FAST simulations of models with different caisson dimensions, along with the regular monopile and the fixed base model, are listed in Table 6.

The results for the tower top displacement show that reductions in caisson dimensions yield larger displacements, as expected.

Figure 11 plots the PSDs of the three caisson models. The PSDs show the expected reductions in natural frequencies for reduced caisson dimensions, especially for the higher modes.

TABLE 6 Maximum and mean values of mudline moment, mudline shear force and tower top displacement from 10-minute FAST simulations of different caisson dimensions

	Mudline Fore-aft Moment, MNm		Mudline Fore-aft Shear Force, MN		Tower-Top Fore-aft Displacement, m	
Caisson Dimensions	Max	Mean	Max	Mean	Max	Mean
15 m x 7.5 m	118.10	67.47	3.683	0.596	0.688	0.486
12 m x 6 m	115.50	67.53	3.652	0.596	0.744	0.511
12 m x 5 m	113.80	67.57	3.634	0.596	0.767	0.520
10 m x 5 m	115.70	67.65	3.615	0.596	0.822	0.548
Monopile	115.80	67.62	3.616	0.596	0.813	0.540
Fixed base	114.50	67.39	3.632	0.598	0.644	0.462

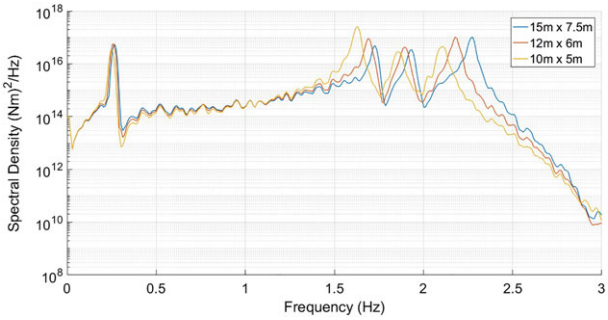

FIGURE 11 PSD from mudline fore-aft bending moment for models with different caisson dimensions [Colour figure can be viewed at wileyonlinelibrary.com]

5 | FATIGUE ANALYSES

In the preceding sections, the only parameters for comparison of the different foundation models have been the output time series. To gain more insight into how these results affect the lifetime of the OWT, fatigue analyses of the different foundation models are carried out in this section using the MATLAB-based tool *MLife*.[51] MLife is developed by NREL, is mainly created to post-process FAST output, and computes statistical information and fatigue estimates for one or more time-series. In addition to accumulated lifetime damage and the time until failure, *damage equivalent loads* (DELs) are useful to characterize fatigue for wind turbines. MLife calculates both short-time DELs based on single timeseries and lifetime DELs based on an entire set of time-series. A DEL is a fluctuating load with constant amplitude and constant frequency, prescribed by the MLife user, causing the same equivalent damage as the stochastic loads from the time series. MLife is used in this section to investigate the difference in fatigue life and DELs between the foundation models studied in the preceding sections.[51]

5.1 | Fatigue in OWTs

Fatigue is the process of gradual damage in materials when they are subjected to cyclic loading.[52] Even though the stresses acting on OWT support structures are far below the yield stress limit of the material, fatigue occurs when small stresses are applied a sufficient number of times. The *Palmgren-Miner rule* predicts fatigue damage under the assumptions of linear cumulative damage and is given as

$$D = \sum_i \frac{n_i}{N_i}, \tag{8}$$

where D is the fatigue damage in the structural component considered, n_i is the number of stress cycles at stress level i, and N_i is the number of cycles to failure at stress level i. Failure occurs when $D \geq 1$.

Wind turbines are often designed for a lifetime of 20 years. Compared with other structures, the contribution of the turbine's self-weight to the stresses is small, while the contribution from bending moment caused by wind and waves is large. The wind turbine structure is subjected to load cycles of the order of 500 million during its lifetime[53] and must be able to withstand these loads without failure. Hence, fatigue is an unavoidable topic when simulating the loads acting on wind turbines.

5.2 | Load conditions and FAST simulations

In IEC 61400-3,[54] a large number of design load cases (DLCs) are specified to be considered when performing fatigue and ultimate load analyzes. The DLCs cover the most significant conditions an OWT may experience, including normal operating conditions, extreme conditions, start-up and shutdown events, fault situations, and parked or idling states. To get a realistic presentation of a typical offshore wind site, the wind and wave conditions from the reference *Project UpWind*[55] are used in this paper. This is an offshore wind site located in the Dutch North Sea, called *K13*, which is a typical shallow site suitable for monopile foundations. Climate data have been measured on this site for 22 years and are described with scatter diagrams including mean wind speed at hub height, significant wave height, and peak spectral period. These values were used in the

TABLE 7 Load cases[55]

Load case	U, m/s	TI, %	Hs, m	Tp, m	f, %
1	2	29.2	1.07	6.03	6.071
2	4	20.4	1.10	5.88	8.911
3	6	17.5	1.18	5.76	14.048
4	8	16.0	1.31	5.67	13.923
5	10	15.2	1.48	5.74	14.654
6	12	14.6	1.70	5.88	14.272
7	14	14.2	1.91	6.07	8.381
8	16	13.9	2.19	6.37	8.316
9	18	13.6	2.47	6.71	4.186
10	20	13.4	2.76	6.99	3.480
11	22	13.3	3.09	7.40	1.534
12	24	13.1	3.42	7.80	0.974
13	26	12.0	3.76	8.14	0.510
14	28	11.9	4.17	8.49	0.202
15	30	11.8	4.46	8.86	0.096
16	32	11.8	4.79	9.12	0.050
17	34-42	11.7	4.90	9.43	0.019

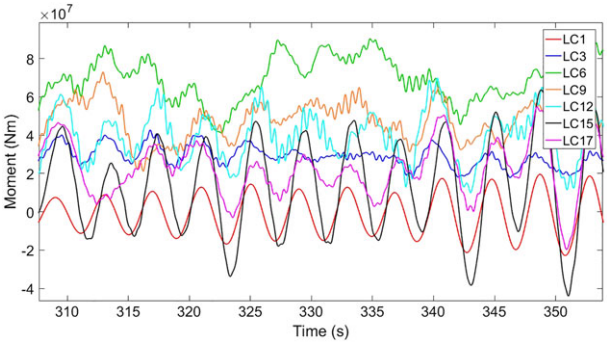

FIGURE 12 Details of mudline for-aft bending moment for selected load cases for the improved AF model monopile [Colour figure can be viewed at wileyonlinelibrary.com]

present analyses. The measurement data are lumped into 17 different load cases (LCs) with different wind and wave combinations and probability of occurrence. The load cases from *K*13 site are presented in Table 7.

In this table, U is the mean wind speed at hub height, and $f(\%)$ is the frequency of occurrence of the load case. The wind speed of the 17*th* load case is set to the mean value, $U = 38$ m/s.

LC2-LC12 from Table 7, where the mean wind is between cut-in (3 m/s) and cut-out (25 m/s) speed, represents *DLC 1.2 Power production* from IEC 61400-3,[54] while LC1, with wind below cut-in speed, and LC13-LC17, with wind above cut-out speed, applies to *DLC 6.4 Parked (standing still or idling)*. It is assumed that the turbine is operating at all times during the design lifetime when the wind speed is between cut-in and cut-out speeds, so LC1 and LC13-LC17 are the only cases where the rotor is idling. The DLCs representing start-up, shut down, and other fault events are not included. This decision was made based on two reasons. Firstly, generating and simulating all the DLCs recommended in IEC 61400-3,[54] including all the possible fault events for every wind speed for every foundation model would be very time consuming. Such detailed analyses are required for real design which is not the objective of this study. Secondly, the main aim of this paper is to compare foundation models; therefore, exciting the different models with the range of environmental loads presented above will give sufficient results for that purpose. The same reasoning lies behind choosing to simulate one wind and wave seed per load case instead of six, as recommended in IEC 61400-3.

Wind fields for the 17 load cases were generated by TurbSim using the Kaimal spectral model and the power law wind profile, as in the previous sections. The hydrodynamic loads were generated by HydroDyn using a JONSWAP spectrum. When the wind speed is higher than the rated wind speed of 11.4 m/s, the initial blade pitch angles and rotor speed increase with wind speed due to the turbine's blade-pitch controller. These were changed in the ElastoDyn file for each load case.

For the nonoperating cases, when the rotor is idling or parked, that is LC1 and LC13-LC17, the rotor speed was set to 0, the generator was turned off, and the blade pitch angles were set to 90° to make them pitched out of the wind.[56-58]

For every foundation model considered, 10-minute simulations of each load case were run in FAST. Figure 12 shows a short time window of the mudline moment time series for a selection of the load cases for the monopile modelled with the improved AF method. As stated by Jonkman,[59] the highest loads are expected to occur at the rated (11.4 m/s) and the cut-out wind speeds. Figure 12 shows that the highest moments occur in LC6, which has a wind speed of 12 m/s, close to the rated speed. However, the largest moment ranges occur at the highest environmental loads plotted, ie, LC15 and LC17. In addition to these cases containing the strongest winds and highest waves, the rotor is idling, which means that the aerodynamic damping is highly reduced, leading to high load amplitudes at the mudline. It is clear that LC1, LC15, and LC17 represent an idling rotor, while the operational natural frequencies are present in LC3, LC6, LC9, and LC12, causing high frequency moment oscillations.

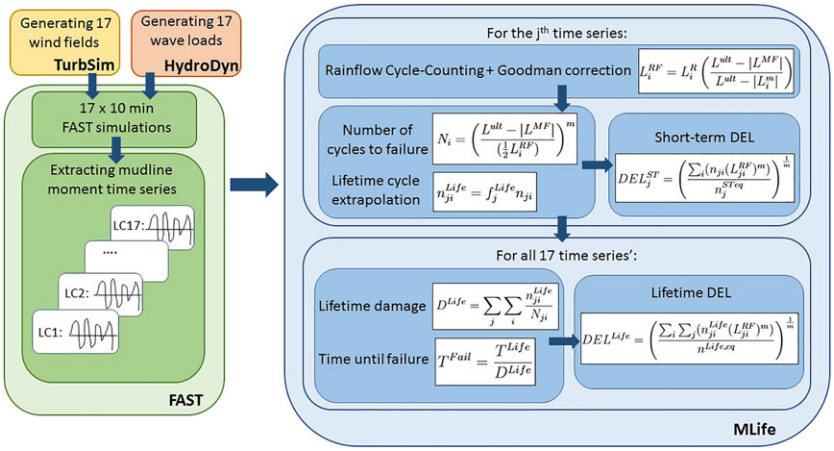

FIGURE 13 Steps of the fatigue analyses[48] [Colour figure can be viewed at wileyonlinelibrary.com]

5.3 | MLife analyses

All the fatigue analyses were based on mudline fore-aft bending moment time series from the FAST analyses of the 17 load cases in Table 7 for each foundation model. The MLife user must specify the scale and shape factors of the Weibull distribution of the wind, which are site dependant, as well as cut-in, cut-out and maximum wind speed to include in the analysis. In addition, a number of other parameters need to be specified in the MLife input file, including the design lifetime, the DEL frequency, the Wöhler exponent m to be used in the S-N curve, the load range binning values, the fixed-mean load, and the ultimate design load L^{ult}.[51] The ultimate load is the highest load that the cross section of the studied component can withstand before failure. Ideally, the ultimate load would be based on an FE analysis of the component, or on data specified for the NREL 5MW. However, as no FE model or data are available, the ultimate tensile strength σ^{ult} of the studied cross section was used as a reference for failure. The ultimate strength of the steel used for the NREL 5MW substructure was assumed to be 440 MPa,[60] and the corresponding value of the ultimate load was calculated to be 7.46×10^8Nm. Based on Det Norske Veritas,[47] $m = 5$ was chosen to be the suitable choice for this analysis. Moreover, the load bin width was set to 100 Nm, and the fixed-mean load was set to *AM*, telling MLife to compute the fixed mean using the aggregate mean across all input files. It was assumed that the turbine is operating at all times during the design lifetime when the wind speed is between cut-in and cut-out speeds. The Weibull scale and shape factors for the *K*12 site are specified by Fischer et al[55] as λ_W=11.31 m/s and k_W=1.97. MLife uses Rainflow Cycle-Counting (RCC) on the load time series to obtain load ranges,and calculates the lifetime damage, D^{Life}, the time until failure, T^{Fail}, and the *DEL*.

MLife fatigue analyses were run for the following foundation models:

- The NREL 5MW fixed base reference model
- Monopile foundation models: The monopile with regular dimensions, the 16-m pile, and the models with reduced pile wall thickness
- Caisson foundation models: 12 m × 6 m model, 15 m × 7.5 m model, and 10 m × 5 m model

In all these models, the substructure has the same cross-sectional properties at the mudline and hence the same ultimate load, except for the models with reduced wall thickness. L^{ult} is proportional to the bending rigidity of the pile. Hence, L^{ult} for the models with $t_w = 0.05$ m and $t_w = 0.04$ m is reduced by 16% and 33%, respectively. It is important to calculate the ultimate load based on cross sectional dimensions, because this is the only input parameter reflecting the properties of the cross section considered.

An overview of the steps of the method for fatigue analyses is illustrated in Figure 13, which covers all the involved elements from load generation in TurbSim and HydroDyn to calculating lifetime damage and DELs in MLife. The results of the analyses are presented and compared in the following section.

5.4 | Results

Table 8 lists the results of the MLife analyses for the different foundation models. The DELs are reported as range values, or peak-to-peak values, with fixed mean values calculated by MLife, fluctuating with a frequency of 1 Hz. The oscillation frequency of the DELs is prescribed by the MLife user and highly affects the load values.

Table 8 shows a significant difference in fatigue life for the fixed base and monopile. Even though the differences in mudline moments discussed in Section 2.3 are not large, 1% increase in maximum moment and 7 % increase in standard deviation, the differences are large enough to strongly affect the fatigue life. The time until failure, or fatigue life, is reduced by 22% when a flexible foundation is introduced. Furthermore, the monopile with a shorter length of 16 m shows almost no difference in fatigue life compared with the original monopile with length 36 m, which underlines the conclusions drawn in Section 3.1 on potentially conservative design.

Moving on to the monopiles with reduced wall thickness, Table 8 shows how important a reduction in wall thickness is for the fatigue life; this is believed to be due to the higher bending stresses. The fatigue life of the model with $t_w = 0.05$ m is reduced to 8.47 years, a reduction of 62%,

TABLE 8 Results from MLife fatigue analyses

Model	Lifetime Damage (–)	Time Until Failure, years
Fixed base	0.700	28.6
Monopile	0.898	22.3
Monopile, L=16m	0.901	22.2
Monopile, t_w=0.05m	2.360	8.5
Monopile, t_w=0.04m	8.270	2.4
Caisson, 15m × 7.5m	0.701	28.5
Caisson, 12m × 6m	0.775	25.81
Caisson, 10m × 5m	0.891	22.5

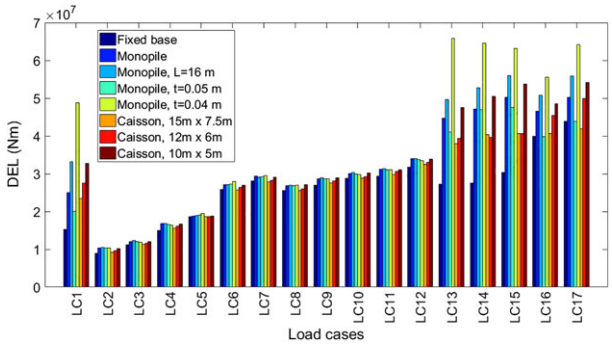

FIGURE 14 Short term DEL for the different load cases [Colour figure can be viewed at wileyonlinelibrary.com]

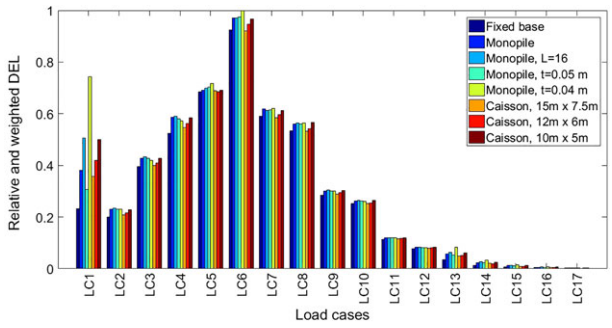

FIGURE 15 Relative short term DEL for the different load cases, weighted with probability of occurrence [Colour figure can be viewed at wileyonlinelibrary.com]

and the model with t_w = 0.04 m has a short fatigue life of 2.42 years, a reduction of 89% Hence, even with the limited analyses on fatigue, it can be concluded that an OWT with a monopile wall thickness of 0.05 or 0.04 m will not live through its expected lifetime of 20 years.

The model with a 10 m × 5 m caisson foundation gives similar MLife results as the monopile, while the 12 m × 6 m caisson has an accumulated fatigue life between the fixed base and the regular monopile, which is expected based on the mudline moment plots in Figure 10 and the maximum moment values from Table 6. The largest caisson gives MLife results very close to the fixed base model, implying that OWTs with caissons of that size can be treated as rigidly connected to the base.

The short-term DELs for each input time series are shown in Figure 14 for the analyzed foundation models.

Figure 14 shows that the highest DELs, and also the largest deviation between the models, occur for LC13-LC17, as expected, due to the high moment amplitudes of these cases. The high DELs for LC1 may seem counter intuitive, as the wind and wave loads are low for this case. However, as was shown in Figure 12, when the rotor is idling and the aerodynamic damping is reduced, the tower is free to oscillate at its first natural frequency, which gives high moment amplitudes despite small maximum values. The largest DELs occur for the model with the smallest wall thickness.

Figure 15 displays the relative DELs, weighted with the load cases' probability of occurrence from Table 7. The load case with the highest DEL and hence the load case contributing the most to the lifetime damage is LC6, due to the combination of the wind speed being close to the turbine's rated wind speed and the high probability of occurrence. The high probability of occurrence of LC1 leads to a large contribution from this case as well, particularly for the monopile with t_w = 0.04 m. Note that the DELs are loads and not stresses, implying that similar DELs give significantly larger fatigue damage for the models with reduced wall thickness.

From these results, it can be concluded that in general, mean winds below cut-in speed and around rated wind speed contribute the most to fatigue damage of an OWT. The difference in DELs between different foundation models are moderate for an operating turbine, but large for mean winds below cut-in and above cut-out speeds when the turbine is idling and damping is low. This points to the importance of consideration of soil damping for more economical design.[23]

6 | CONCLUSIONS

Based on the analyses carried out in this paper, the following conclusions can be drawn:

- Neglecting the effect of the foundation in the OWT model, like the fixed base default model in FAST, gives inaccurate and underestimated results for the structural dynamic response and fatigue damage. A significant reduction in fatigue life of 22% was observed for the flexible foundation model compared with the fixed base model.
- The method chosen for modelling the OWT foundation is important to obtain a correct representation of the structural dynamic response. The effect of the off-diagonal terms in the soil-foundation stiffness matrix at the mudline plays an important role when modelling the foundation flexibility. Disregarding the off-diagonal terms in the simplified apparent fixity model in Section 2.1 gave a foundation model that was too soft and lead to over-predictions of the loads and displacements in the substructure. Including the whole stiffness matrix, implemented in the improved AF model in Section 2.2, leads to a stiffer foundation model and gave a significant difference in structural response compared with the simplified method.
- Reductions of the monopile length for the cases considered have almost no effect on the FAST results, due to minimal changes in soil-pile stiffness coefficients from the soil-profile considered. A reduction from 36 to 26 m leads to no noticeable difference, and the length had to be reduced to 16 m for a small differences to appear.
- A small reduction of the monopile wall thickness leads to a moderate increase in bending moments, but a large increase in fatigue damage, and hence a large reduction in fatigue life. Designing the NREL 5MW with a wall thickness smaller than 0.06 m will probably lead to premature failure, either by fatigue or possibly by buckling.
- A caisson foundation with a diameter of 10 m and a depth of 5 m gives similar dynamic response and fatigue life as the regular monopile with length 36 m and diameter 6 m with the assumptions made and modelling methods used in this paper.
- Capacity analyses of the soil-foundation system would have to be carried out in addition to the analyses presented in this paper in order to conclude on possibilities of dimension reduction. Buckling is especially of concern for the monopile models with reduced wall thickness and for the caisson models.
- The fatigue damage calculations in MLife are highly dependent on input parameters, especially the Wöhler exponent and the ultimate load. For the NREL 5MW, there are no recommended values to use for the ultimate load when an FE model is not available, and research on the topic provides a wide range of alternatives. This has to be taken into consideration when evaluating the values of the resulting fatigue damage and when comparing the results to previous research. Without knowing the exact values for the input parameters, in addition to only simulating one wind and wave seed for each load case, the MLife fatigue analysis will produce results suitable for comparison, as demonstrated in this paper, but may not give exact values of the fatigue life for the component considered.[53]
- It should be noted that the analyses and results presented in this paper are for a certain set of soil, foundation, and structural parameters. Therefore, some of the conclusions may not be generalized to all OWT configurations and sizes.

ACKNOWLEDGEMENT

This paper is based partly on the first author's Master's thesis at the Department of Structural Engineering, Norwegian University of Science and Technology (NTNU).[48]

ORCID

Amir M. Kaynia https://orcid.org/0000-0002-7774-3860

REFERENCES

1. International Renewable Energy Agency. Offshore innovation widens renewable energy options. ISBN: 978-92-9260-079-2; 2018.
2. Global Wind Energy Council. Global Wind Statistics 2016; 2017.
3. Passon P, Kühn M. State-of-the-art and development needs of simulation codes for offshore wind turbines. *Endowed Chair of Wind Energy (SWE),Univ Stuttgart*. 2005:1-11.
4. Lombardi D, Bhattacharya S, MuirWood D. Dynamic soil-structure interaction of monopile supported wind turbines in cohesive soil. *Soil Dyn Earthq Eng*. 2013;49:165-180.
5. Bloomberg New Energy Finance. Global Trends in Renewable Energy Investment, Report. Frankfurt School of Finance and Management; 2017.
6. Kausel E. Early history of soil-structure interaction. *Soil Dyn Earthq Eng*. 2010;30:822-832.
7. Kourkoulis RS, Lekkakis PC, Gelagoti FM, Kaynia AM. Suction caisson foundations for offshore wind turbines subjected to wave and earthquake loading: effect of soil-foundation interface. *Géotechnique*. 2014;64(3):171-185.
8. Skau KS, Grimstad G, Page AM, Eiksund GR, Jostad HJ. A macro-element for integrated time domain analyses representing bucket foundations for offshore wind turbines. *Mar Struct*. 2018;59:158-178.

9. Novak M, Nogami T. Soil-pile interaction in horizontal vibration. *Earthq Eng Struct Dyn*. 1977;5(3):263-281.
10. Kaynia AM. Characteristics of the dynamic response of pile groups in homogeneous and nonhomogeneous media. In: Proc. 9th World Conference of Earthquake Engineering, Vol. 3; 1988; Tokyo-Kyoto, Japan:575-580.
11. Kaynia AM, Kausel E. Dynamics of piles and pile groups in layered soil media. *Soil Dyn Earthq Eng*. 1991;10(8):386-401.
12. Winkler E. *Die Lehre von Elasticzitat und Festigkeit (On Elasticity and Fixity)*. Czech Republic: Prague; 1867.
13. API Recommended Practice for Planning. Designing and Constructing Fixed Offshore Platforms—Working Stress Design American Petroleum Institute; 2011.
14. Zaaijer MB. Foundation modelling to assess dynamic behaviour of offshore wind turbines. *Appl Ocean Res*. 2006;28:45-57.
15. Bush E, Manuel L. Foundation models for offshore wind turbines Erica. In: 47th AIAA Aerospace Sciences Meeting Including The New Horizons Forum and Aerospace Exposition; 2009; Orlando, Florida.
16. Klikvort RT. Centrifuge modelling of drained lateral pile-soil response. *PhD Thesis*; 2012.
17. Boulanger RW, Curras CJ, Kutter BL, Wilson DW, Abghari A. Seismic soil-pile-structure interaction experiments and analyses. *J Geotech Geoenviron Eng*. 1999;125(9):750-759.
18. Taciroglu E, Rha CS, Wallace JW. A robust macroelement model for soil-pile interaction under cyclic loads. *J Geotech Geoenviron Eng*. 2006;132(10):1304-1314.
19. Fatigue SS. Extreme wave loads on bottom fixed offshore wind turbines. Effects from fully nonlinear wave forcing on the structural dynamics. *PhD thesis*: DTU Wind Energy; 2013.
20. Zania V. Foundation models for offshore wind turbines. In: Proceedings of the 9th International Conference on Structural Dynamics EURODYN, Vol. 2014. Porto; 2014; Portugal.
21. Ziegler L, Voormeeren S, Schafhirt S, Muskulus M. Sensitivity of wave fatigue loads on offshore wind turbines under varying site conditions. *Energy Procedia*. 2015;80:193-200.
22. Markou AA, Kaynia AM. Nonlinear soil-pile interaction for offshore wind turbines. *Wind Energy*. 2018;21:558-574. https://doi.org/10.1002/we.2178
23. Aasen S, Page AM, Skau KS, Nygaard TA. Effect of foundation modelling on the fatigue lifetime of a monopile-based offshore wind turbine. *Wind Energy Sci*. 2017;2:361-376.
24. Iwan VL. On a class of models for the yielding behavior of continuous and composite systems. *J Appl Mech*. 1967;34(3):612-617.
25. Krathe VL, Kaynia AM. Implementation of a non-linear foundation model for soil-structure interaction analysis of offshore wind turbines in FAST. *Wind Energy*. 2017;20(4):695-712.
26. Jonkman JM, Buhl ML. FAST User's Guide National Renewable Energy Laboratory; 2005.
27. Bisoi S, Haldar S. Dynamic analysis of offshore wind turbine in clay considering soil-monopile-tower interaction. *Soil Dyn Earthq Eng*. 2017;63:19-35.
28. Carswell W, Johansson J, Løvholt F, Arwade AR, Madshus DG. Foundation damping and the dynamics of offshore wind turbine monopiles. *Renew Energy*. 2015;80:724-736. doi:https://doi.org/10.1016/j.renene.2015.02.058
29. Bayat M, Andersen LV, Ibsen LB. p-y-y curves for dynamic analysis of offshore wind turbine monopile foundations. *Soil Dyn Earthq Eng*. 2016;90:38-51.
30. Aasen S. Soil-structure interaction modelling for an offshore wind turbine with monopile foundation. *MS Thesis*; 2016.
31. Damgaard M, Zania V, Andersen LV, Ibsen LB. Effects of soil-structure interaction on real time dynamic response of offshore wind turbines on monopiles. *Eng Struct*. 2014;75:388-401.
32. Andersen LV, Vahdatirad MJ, Sichani MT, Sørensen JD. Natural frequencies of wind turbines on monopile foundations in clayey soils—a probabilistic approach. *Comput Geotech*. 2012;43:1-11.
33. Pais A, Kausel E. Approximate formulas for dynamic stiffnesses of rigid foundations. *Soil Dyn Earthquake Eng*. 1988;7(4):213-227. https://doi.org/10.1016/S0267-7261(88)80005-8
34. Doherty JP, Houlsby GT, Deeks AJ. Stiffness of flexible caisson foundations embedded in nonhomogeneous elastic. *soil J Geotech Geoenviron Eng*. 2005;131(12):1498-1508. https://doi.org/10.1061/(ASCE)1090-0241(2005)131:12(1498)
35. Liingaard M, Andersen L, Ibsen LB. Impedance of flexible suction caissons. *Earthquake Eng Struct Dyn*. 2007;36(14):2271. https://doi.org/10.1002/eqe.737
36. Gelagoti F, Lekkakis P, Kourkoulis R, Gazetas G. Estimation of elastic and non-linear stiffness coefficients for suction caisson foundations. In: Proc., XVI European Conf. on Soil Mechanics and Geotechnical Engineering. ICE Publishing; 2015; London.
37. He R, Pak RYS, Wang LZ. Elastic lateral dynamic impedance functions for a rigid cylindrical shell type foundation. *Int. J. Numer. Anal. Methods Geomech*. 2017;41(4):https://doi.org/10.1002/nag.2567.
38. Efthymiou G, Gazetas G. Elastic stiffnesses of a rigid suction caisson and its cylindrical sidewall shell. *ASCE J Geotech Geoenviron Eng*. 2019;145(2). https://doi.org/10.1061/(ASCE)GT.1943-5606.0002013
39. NWTC Information Portal (FAST v8). National Renewable Energy Laboratory. https://nwtc.nrel/gov/FAST8 Accessed February; 2017.
40. Bir G. User's Guide to BModes (Software for Computing Rotating Beam Coupled Modes). *Natl Renewable Energy Lab*. 2007:21.
41. Jonkman J, Butterfield S, Musial W, Scott G. Definition of a 5-MW reference wind turbine for offshore system development tech. https://doi.org//10.1002/ajmg.10175; 2009.
42. Jonkman JM, Musial W. IEA Wind Task 23, Offshore Wind Technology and Deployment. Subtask 2 The Offshore Code Comparison Collaboration (OC3); 2010.
43. Passon P. Derivation and Description of the Soil-Pile-Interaction Models University of Stuttgart; 2006.
44. Bush E, Agarwal P, Manuel L. The influence of foundation modeling assumptions on long-term load prediction for offshore wind turbines. In: ASME 27th International Conference on Offshore and Arctic Engineering. OMA; 2008:2008-57893.
45. Kaynia AM. *Dynamic Stiffness and Seismic Response of Pile Groups*. Cambridge: MIT; 1982.
46. Vesic AB. Bending of beams resting on isotropic elastic solid. *J Soil Mech Found Eng*. 1961;87:35-53.
47. Det Norske Veritas. DNV-OS-J101 Design of Offshore Wind Turbine Structures; 2014.
48. Løken IB. Dynamic Response and Fatigue of Offshore Wind Turbines. *MS Thesis*: Norwegian University of Science and Technology; 2017.

49. Tassoulas J. *Elements for Numerical Analysis of Wave Motion in Layered Media*. Cambridge: MIT; 1981.
50. Madsen S, Andersen L, Ibsen L. Numerical buckling analysis of large suction caissons for wind turbines on deep water. *Engineering Structures*. 2013;57:443-452. ISSN: 01410296.
51. Hayman GJ, Buhl M. MLife Theory Manual for Version 1.00 tech. *Natl Renewable Energy Lab*. 2012.
52. Der Tempel JV. Design of Support Structures for Offshore Wind Turbines. *PhD thesis*: Technische Universiteit Delft; 2006.
53. Schaffarczyk A. *Understanding Wind Power Technology: Theory, Deployment and Optimisation*. John Wiley and Sons Ltd; 2014.
54. 61400-3, N E K I E C, Wind Turbines - Part 3: Design requirements for offshore wind turbines. Norwegian Electrotechnical Publication; 2009.
55. Fischer T, de Vries W, Schmidt B. Upwind Design Basis WP4: Offshore Foundations and Support Structures Project Upwind; 2010.
56. Jonkman J. Overview of the ElastoDyn Structural-Dynamics Module. *Natl Renewable Energy Lab*. 2013.
57. Jonkman JM, Hayman GJ, Jonkman BJ, Damiani RR. AeroDyn v15 User's Guide and Theory Manual National Renewable Energy Laboratory; 2016.
58. Jonkman J. Overview of the ServoDyn Control and Electrical-Drive Module National Renewable Energy Laboratory; 2014.
59. Jonkman JM. Dynamics Modeling and Loads Analysis of an Offshore Floating Wind Turbine National Renewable Energy Laboratory; 2007.
60. Det Norske Veritas. DNV-OS-B101 - Metallic Materials; 2012.

How to cite this article: Løken IB, Kaynia AM. Effect of foundation type and modelling on dynamic response and fatigue of offshore wind turbines. *Wind Energy*. 2019;22:1667–1683. https://doi.org/10.1002/we.2394